ELSEVIER

Journal of Nuclear Materials 241–243 (1997) 299–304

journal of nuclear materials

Modelling of transition from attached to detached state and self-consistent calculations of He levels in ITER

M. Sugihara [a,*], T. Amano [a,b], D. Boucher [c], Y. Igitkhanov [a], G. Janeschitz [a], H.D. Pacher [d], D. Post [a,c], P. Yushmanov [e]

[a] *ITER Joint Central Team, D-85748 Garching, Germany*
[b] *National Institute of Fusion Science, Nagoya, Japan*
[c] *ITER Joint Central Team, San Diego, CA, USA*
[d] *The NET Team, D-85748 Garching, Germany*
[e] *University of California, San Diego, CA, USA*

Abstract

This paper describes models that address both power and particle control with the ITER divertor. For power control, the characteristics of the transition from attached to detached divertor operation are studied with an extension of our previous simple model [Y. Igitkhanov et al., 22nd EPS, Bournemouth (1995) p. IV-317]. This new model has been applied to JET experiments to show that the model can reproduce global features of the transition. The model has been applied to ITER to identify the range for detached operation in terms of the heating power, upstream density, and impurity level, and the relation between divertor control and core plasma conditions. For particle control, we use the PRETOR transport code together with a two point divertor model [K. Borrass and G. Janeschitz, Nucl. Fusion 34 (1994) 1203] for the edge boundary conditions to study the sensitivity of the central helium concentration to the pumping speed and helium enrichment in the divertor.

Keywords: ITER; Poloidal divertor; Analytical model; Detached plasma; Helium exhaust and control

1. Introduction

We address the two issues of power exhaust and the determination of the operating range for plasma detachment, including the 1D effects and volume recombination, and particle control and the required helium pumping using the same basic physics. Since a unified model for both these issues is not yet available, we have developed two slightly different models to obtain some preliminary results for these issues. The power exhaust issues is addressed with a simple 0D model, which includes models for neutral transport and momentum transfer. The 0D model is supplemented by a 1D model to identify the effects of distributed ionization losses and recombination. The particle control model includes helium and plasma transport in the core and boundary condition which includes the effects of pumping and recycling in the divertor. These models allow us to make parameter scans and estimate the operational space for ITER.

2. Modelling of transition from attached to detached states

2.1. Simple 0D model

The simple 0D model is an extended version of [1]. Two regions are defined: the radiation region and the cushion. In the radiation region, energy is lost by impurity radiation. The power is transported by parallel heat conduction, which is valid except very close to the cushion. In the cushion, the plasma is cold and the remaining power is so small that ionization is excluded. The temperature is taken to be constant within the region ($T_1 = T_w$), and convection determines the heat flow. The location of the

* Corresponding author.

PII S0022-3115(96)00518-1

cushion interface develops self-consistently according to the energy, particle and momentum balance equations. In the cushion, neutrals provide momentum loss, reducing the pressure below that of the attached state. The following seven equations for seven unknown variables $\Gamma_{\|}$, q_w, T_w, T_{up}, n_0, L_m and f_m are solved for specified values of the up-stream density n_{up} and power q_{up} and impurity level f_z [1]:

(1) The particle flux at the plate $\Gamma_{\|}$ (s^{-1} m^{-2}):

$$\Gamma_{\|} = c_{s0}(1 - f_m)\frac{n_{up}T_{up}}{4k\sqrt{T_w}} \tag{1}$$

(2) The remaining power flow q_w (W/m^2) transferred to the plate by convection:

$$q_w = \Gamma_{\|}k(\varepsilon + \gamma T_w) \tag{2}$$

(3) The momentum loss fraction f_m due to charge exchange [3]:

$$f_m = 1 - \exp(-L_m/\lambda^*) \tag{3}$$

(4) Particle flux conservation for neutrals n_0 and ions ($\langle\,\rangle$ means average of decay factor by ionization for neutrals generated from various part of divertor plate):

$$\Gamma_{\|}\langle\exp(-\Delta/\lambda_{ion})\rangle A_1 = \frac{B_{\|}}{B_p}n_0\left(C_{pump} + \tfrac{1}{4}A_0\nu_0\eta\right),$$

$$A_1 = 2\pi R\Delta \tag{4}$$

(5) Heat conduction in the radiation region:

$$q^2(T) = q_w^2 + \tfrac{1}{2}\chi_0 p_{up}^2 f_z\int_{T_w}^{T}\sqrt{T}\,L(T)\,dT \tag{5}$$

(6) The length of the radiation zone, L_r (L_0 being the connection length between X-point and divertor strike point):

$$L_r = \chi_0\int_{T_w}^{T_{up}}\frac{T^{5/2}}{q(T)}dT = L_0 - L_m \tag{6}$$

(7) Cold neutral penetration into the center of the cushion at the interface between the radiation zone and the cushion (width of Δ_c):

$$\lambda_{ion} = \Delta_c \tag{7}$$

imposed to ensure that the basic assumption of Eq. (3) is satisfied, i.e., that charge exchange with cold neutrals removes the momentum from the plasma.

2.1.1. Comparison with JET experiments

The model has been validated by matching the behaviour of particle flux in D_2 and N_2 puffing experiments in JET (shot No. 33204) [4], for which the ion saturation current shows a typical roll-over with time (main plasma density and total radiation increases). The simulations are compared in Fig. 1 with the experimental results (the vertical bar shows the range of the flux on inner and outer

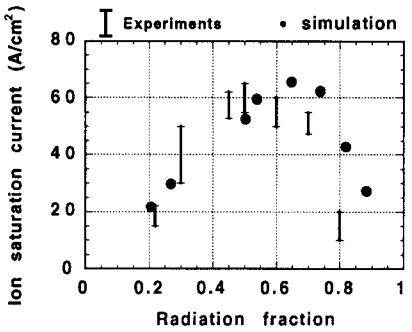

Fig. 1. Comparison of ion saturation current obtained by simple model with JET experiments as a function of total radiation fraction.

divertor plate). The two major uncertainties in the simulation are the impurity level in the divertor region and the radiation partition between main plasma and divertor. We assumed a radiation partition of 1:1 for main: divertor for a radiation fraction of 0.2. Then the impurity level is adjusted to match the radiation level using an impurity radiation rate enhanced to account for recycling and charge exchange recombination effects. This level is assumed constant during the rest of the discharge. The global features of the transition can be simulated reasonably. Some of the discrepancy in the roll-over point and the faster reduction of the particle flux after the transition can be removed by inclusion of recombination, as shown in Section 2.2 and in [5].

2.1.2. ITER solutions

The features of the transition in ITER are shown in Fig. 2 as a function of the upstream density. The upstream heat flux is 650 MW/m^2 during burn. The connection length is

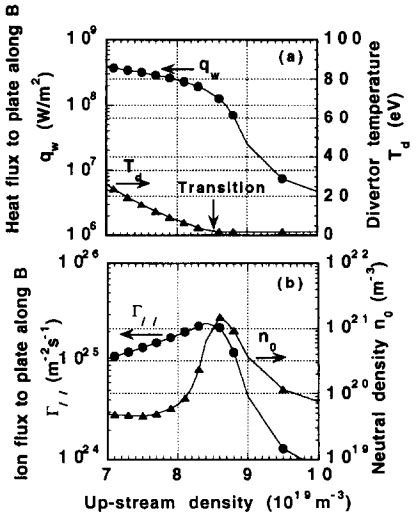

Fig. 2. Transition features of ITER from attached to detached as upstream density increases. (a) Heat flux q_w on plate and divertor temperature T_d. (b) Particle flux $\Gamma_{\|}$ and neutral density n_0.

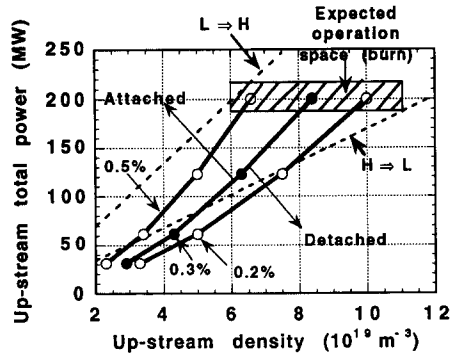

Fig. 3. Operation space of divertor detachment for various Ar impurity level (thick solid lines). Expected operation region for burn is shown (hatched). Also shown are transition threshold condition between L and H mode.

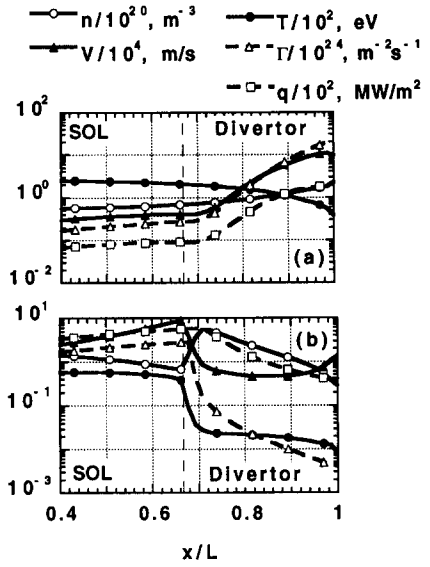

Fig. 4. Spatial plasma profiles along magnetic field lines for attached case (a); $n_{up} = 7 \cdot 10^{19}$ m^{-3}, $f_z = 0.3\%$; and for detached case (b); $n_{up} = 1 \cdot 10^{20}$ m^{-3}, $f_z = 0.35\%$.

$L_0 = 40$ m. A constant concentration of 0.3% Argon is assumed and as in the JET cases, an enhanced emissivity [6] is used.

The transition occurs when the divertor temperature reaches 2–3 eV (detached region starts to be formed) and the heat flux drops sharply as shown in Fig. 2a. The particle flux shows a roll-over (Fig. 2b). The neutral density increases toward the transition (high recycling) and decreases beyond the transition as the particle flux decreases.

The Ar impurity levels and upstream total powers were varied to find the upstream density necessary for detachment (Fig. 3). Detached operation can be obtained for 0.2–0.5% argon for various discharge phases (heating with density ramp-up and burn). During burn (at high density and constant fusion power), f_z can be reduced, while maintaining detachment, since the radiation losses increase with n^2 while the H-to-L transition threshold power increases with n^1. Main plasma radiation reduces the impurity level and/or upstream density required to achieve detachment.

2.2. 1D divertor model

A 1D divertor model has been developed to check the applicability of the simple 0D model. The 1D model solves fluid equations for plasma parameters n, v and T ($T_e = T_i$) along field lines. Cross field terms are introduced as source terms averaged across the plasma. Volume recombination (radiative and three body) is included. Realistic radiation emissivities are used. The convection and conduction-dominated regions are not separated and are treated simultaneously. Friction of plasma flow with neutrals surrounding the plasma column is included to simulate the parallel momentum loss. The same neutral model as in the 0D model is employed. Impurities are distributed proportional to plasma density. Calculations are performed for typical ITER conditions: Input heat flux $Q_\perp = 150$ MW, particle flux about $4–7 \cdot 10^{23}$ s^{-1} and a connection length between mid-plane and divertor plate = 150 m.

In the attached case (Fig. 4a) the neutral density around the plasma is too small to ensure efficient momentum removal, and the pressure drop is negligible. Nevertheless 0.3% of Ar and high hydrogen recycling at the plate (95%) can radiate almost 30% of the total energy. In the deeply detached case (Fig. 4b), a strong temperature gradient develops near the X-point. Neutrals around the plasma ensure a significant pressure drop by about an order of magnitude from mid-plane to the target. Almost all the energy is radiated by impurities. The global characteristics of the transition from the attached to the detached state are similar to those of the 0D model, and transition occurs in the same range of upstream density and impurity concentration (Fig. 5). Compared with the 0D result (Fig. 2b), the neutral density is higher and the reduction of particle flux

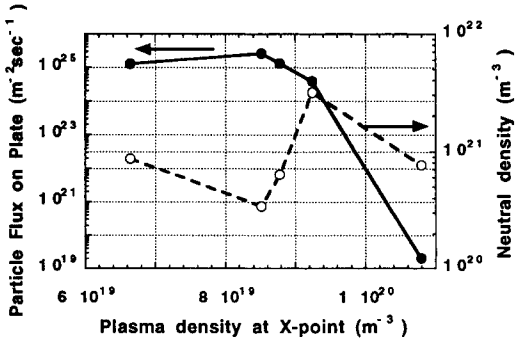

Fig. 5. Particle flux and neutral density versus upstream density at X-point.

is stronger in the 1D model especially when the plasma goes deeply into detached state, which can be attributed to volume recombination [5].

3. He exhaust studies for detached plasmas

The central helium concentration in ITER strongly affects the plasma performance. Decreasing the central helium concentration by 1% is equivalent to adding 0.5 MA of plasma current for plasma confinement. 1.5 GW of fusion power in ITER produces 5×10^{20} He atoms per second which must be removed by the pumping system in the divertor. The helium ions first diffuse from the center to the plasma edge, transport along the scrape-off layer to the divertor and then recombine at the plate and enter the pump as neutral atoms (Fig. 6). To model this complicated process, we have simplified the model in Section 2.1 to develop a self-consistent two-point [2,7] model for the divertor pumping with detached or semi-detached plasmas to use as a boundary condition with the PRETOR tokamak transport code [7]. The helium production and helium transport from the plasma core to the plasma edge are modeled self-consistently in the PRETOR transport code. The two point model is used to provide edge temperature and diffusion flux boundary conditions for the PRETOR code which are consistent with the plasma and neutral conditions in the divertor, including the effects of the plasma pumping system. The effects of plasma and neutral transport in the scrape-off layer and divertor, including effects such as the thermal force, are parameterized by using an assumed 'He enrichment' factor,

$$f_{\mathrm{He}} \equiv \left(\frac{n_{\mathrm{He}}}{2n_{\mathrm{H}_2}+n_{\mathrm{He}}}\right)_{\text{pump duct}} \Bigg/ \left(\frac{n_{\mathrm{He}}}{n_{\mathrm{e}}}\right)_{\text{main plasma edge}}$$

to relate the helium concentration at the plasma edge to the helium concentration in the pump duct (H_2 represents all hydrogenic species).

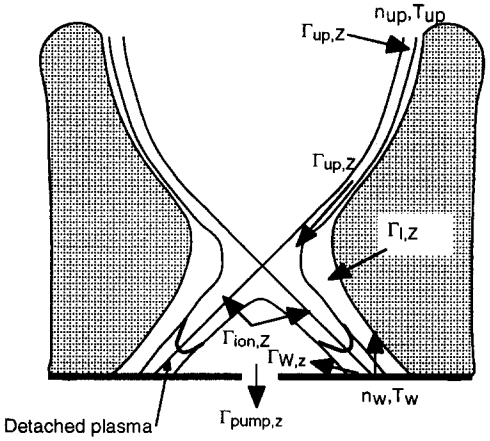

Fig. 6. Divertor configuration.

To relate the plasma conditions and fluxes in the divertor and at the main plasma edge, we begin with the two-point divertor model described in Eqs. (1), (2) and (4), together with a parameterization of the momentum loss and radiation losses as fixed fractions [2] with standard sheath boundary conditions and Bohm perpendicular heat transport. The densities of the hydrogenic and helium ions at the mid-plane plasma edge in terms of the divertor pumping speed and other divertor conditions are determined with a model for divertor recycling and pumping model based on balancing the instantaneous fluxes for fuelling, pumping, recycling and ionization (Fig. 6) in the divertor and the scrape-off layer. The plasma particle flux onto the divertor plate, $\Gamma_{\mathrm{W,Z}}$, is given by $\Gamma_{\mathrm{W,Z}} = \Gamma_{\mathrm{up,Z}} + \Gamma_{\mathrm{ion,Z}}$ where the suffix Z denotes the particle species (D, T or He), $\Gamma_{\mathrm{up,Z}}$ is the plasma particle flux from the main plasma and $\Gamma_{\mathrm{ion,Z}}$ is the recycling flux ionized in the divertor. The total flux on the plate $\Gamma_{\mathrm{W,Z}}$ is determined by the divertor plasma conditions using the sheath boundary conditions.

To calculate neutral fluxes in the divertor, we assume that all the neutral flux from the divertor plate escapes to the private flux region without ionization because the divertor plasma is detached and the ionization rate near the plate is low. Then, we can balance the fluxes from the plate, $\Gamma_{\mathrm{W,Z}}$, and from fuelling, $\Gamma_{\mathrm{I,Z}}$, with the flux being pumped by the plasma due to ionization, $\Gamma_{\mathrm{ion,Z}}$, and by the pump, $\Gamma_{\mathrm{pump,Z}}$: $\Gamma_{\mathrm{W,Z}} + \Gamma_{\mathrm{I,Z}} = \Gamma_{\mathrm{ion,Z}} + \Gamma_{\mathrm{pump,Z}}$. The pumping rates are determined by effective areas so that $\Gamma_{\mathrm{ion,Z}}$ and $\Gamma_{\mathrm{pump,Z}}$ are given by:

$$\Gamma_{\mathrm{pump,Z}} = \frac{A_{\mathrm{pump,Z}}}{A_{0,\mathrm{Z}} + A_{\mathrm{pump,Z}}}(\Gamma_{\mathrm{W,Z}} + \Gamma_{\mathrm{I,Z}})$$

$$\text{and} \quad \Gamma_{\mathrm{ion,Z}} = \frac{A_{0,\mathrm{Z}}}{A_{0,\mathrm{Z}} + A_{\mathrm{pump,Z}}}(\Gamma_{\mathrm{W,Z}} + \Gamma_{\mathrm{I,Z}})$$

where $A_{0,\mathrm{Z}}$ and $A_{\mathrm{pump,Z}}$ are the effective pumping areas of the plasma and the pump given by $A_{0,\mathrm{Z}} = 2\pi R_0 l(1 - \alpha_{\mathrm{Z}})$ and $A_{\mathrm{pump,Z}} = C_{\mathrm{pump}}/(v_{\mathrm{th,Z}}/4)$, respectively where l is the length of the ionizing plasma surface in the divertor, α_{Z} is the albedo of the divertor plasma to neutrals determined by the ratio of charge exchange to ionization processes, C_{pump} is the speed of the pumping system and $v_{\mathrm{th,Z}}$ is the thermal speed of the gas corresponding to 300 K.

The PRETOR code needs the density and temperature at the main plasma edge for boundary conditions. We use Eq. (1) to link the density at the midplane with the plasma flux on the divertor plate. The pumped flux, $\Gamma_{\mathrm{pump,Z}}$, is equal to the flux from the main plasma, $\Gamma_{\mathrm{up,Z}}$, and the fuelling flux, $\Gamma_{\mathrm{I,Z}}$: $\Gamma_{\mathrm{up,Z}} = \Gamma_{\mathrm{pump,Z}} - \Gamma_{\mathrm{I,Z}}$. We can then express the pumped flux in terms of the flux on the plate determined by the sheath conditions and the relations between the upstream density and temperature and the divertor plate flux and temperature using Eqs. (1) and (2) and the model in Ref. [2].

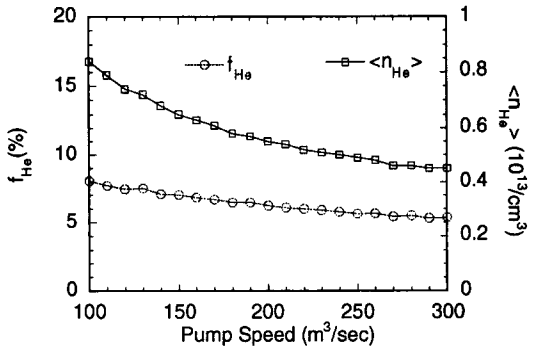

Fig. 7. The averaged He concentration f_{He} and the average He density versus pumping speed.

For ITER, we used a momentum loss fraction, f_m, of 0.8, a divertor plasma temperature at the plate, T_w, of 3 eV, a connection length, L, of 100 m, and an effective pumping area for the plasma, $A_{0,Z}$, of 50 m^2. To fuel the central plasma and replace the fuel that is burned, we used 2 mm pellets injected with a velocity of 2 km/s. The pellet injection rate is feedback controlled to obtain the desired fusion power (1.5 GW).

This model has been used to make a preliminary assessment of the dependence of the central He fraction on the pumping speed and He enrichment factor. For a helium enrichment factor of 0.5, the average He density in the main plasma decreases from $\sim 0.8 \times 10^{19}$ to 0.45×10^{19} m^{-3} and the central helium fraction decreases from 8% to 5% as the pumping speed varies from 100 m^3/s to 300 m^3/s (Fig. 7). The central average helium density decreases with either an increase in the pumping speed or He enrichment. The central average He concentration decreases less rapidly than the density because the total plasma density required to sustain 1.5 GW of fusion power and the relative pumping efficiency for He decrease with lower He densities.

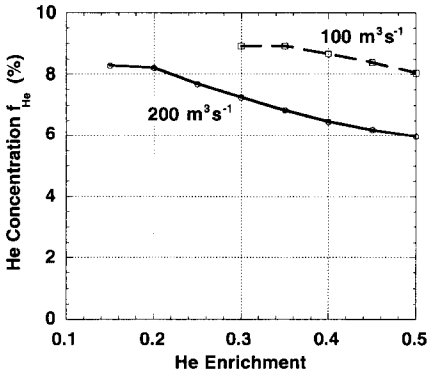

Fig. 8. The average central He concentration f_{He} as function of the He enrichment (ratio of the He concentration in the pump duct to the He concentration at the main plasma edge) for pumping speeds of 100 and 200 m^3/s.

For a pumping speed of 200 m^3/s, the average helium concentration decreases from 8.3% to 6% as f_{He} varies from 0.15 to 0.5 (Fig. 8). For 100 m^3/s, the average helium concentration is greater. This self consistent model indicates that the reference assumption of a helium concentration of about 10% is reasonably conservative, and that lower concentrations may be achievable.

4. Conclusions

Our improved 0D model can reproduce many of the global features of the transition observed on JET experiments. We have used the model for ITER to identify the detached divertor operation space (power and density for various Argon impurity levels), and to obtain an initial indication of the relation between detached divertor and core plasma operation.

Results from the 1D model show that the global characteristics of the transition from the attached to the detached state are similar to those of the simple 0D model, and that the transition occurs in the same range of upstream density and impurity concentration. The neutral density and particle flux are also in the same range. These results support the general adequacy of the simple model. However, reduction of particle flux by recombination is significant, especially when the plasma goes deeply into the detached state, indicating that a 1D model is required [5].

The He recycling model indicates that the central He concentration depends, as expected, on the pumping speed and the helium enrichment. For the parameters expected for ITER, a pumping speed of up to 200 m^3/s and helium enrichment of 0.2 to 0.5, the central He fraction is between 6 and 9%, which will allow adequate He exhaust and central helium fractions consistent with long pulse ignited operation in ITER.

Acknowledgements

This report has been prepared as an account of work performed under the Agreement among the European Atomic Energy Community, the Government of Japan, the Government of the Russian Federation, and the Government of the United States of America on Cooperation in the Engineering Design Activities for the International Thermonuclear Experimental Reactor ('ITER EDA Agreement') under the auspices of the International Atomic Energy Agency (IAEA).

References

[1] Y. Igitkhanov et al., 22nd EPS, Bournemouth (1995) p. IV-317.
[2] K. Borrass and G. Janeschitz, Nucl. Fusion 34 (1994) 1203.

[3] Y. Igitkhanov et al., 21st EPS, Montpellier, Vol. 18B, part II (1994) p. 714.
[4] G. Vlases, ITER Divertor Expert Group Meet., Naka, Oct. 1995.
[5] K. Borrass et al., these Proceeedings, p. 250.
[6] D. Post, J. Nucl. Mater. 220–222 (1995) 143.
[7] D. Boucher et al., Proc. IAEA Tech. Comm. Meet. on Advances in Simulations and Modelling of Thermonuclear Plasmas, Montreal (1992) p. 142.